

Ferromagnetic properties in Fe-doped ZnS thin films

FENG ZHU^{*a}, SHAN DONG^a, GUANDONG YANG^a

^a State Key Laboratory for Superlattices and Microstructures, Institute of Semiconductors, Chinese Academy of Sciences, P. O. Box 912, Beijing 100083, China

Fe-doped ZnS single-phase thin films showing ferromagnetism have been successfully prepared by metal-organic chemical vapor deposition (MOCVD) on GaAs substrates. Field and temperature dependent magnetization curve indicate that the sample with a Curie temperature T_c as high as 270K. The X-ray diffraction and atomic force microscopy (AFM) reveal that the thin films are well crystallized, Fe ions are substituted for Zn ions in the ZnS matrix and no trace of secondary phases or Fe clusters is detected. The experimental results are explained theoretically by spin-polarized density functional calculations within generalized-gradient approximations (GGA), which indicates the observed high T_c could be mainly ascribed to the p - d exchange coupling between Fe ions and host elements.

(Received November 22, 2010; accepted November 29, 2010)

Keywords: Fe-doped ZnS, First principles calculation, Ferromagnetic properties, High Curie temperature

1. Introduction

Transition-metal (TM) doped wide gap II-VI semiconductors materials, such as ZnO, GaN and ZnS, have been extensively investigated for potential magneto-electronic or magneto-optical applications with the purpose of realizing of a high Curie temperature (T_c) [1-6]. Such TM-doped semiconductors called “dilute magnetic semiconductor” (DMS) could be integrated with conventional semiconductor devices for spintronic applications. In past years, many works have studied the doping properties of ZnS [7-11]. For example, Kryshtab *et al* [7] have studied the influence of Cu and Al co-doping on ZnS thin films for structural and luminescent investigations. Mandal *et al* [8] have prepared nanocrystalline ZnS films by high pressure magnetron sputtering and observed that different thickness (10-40nm) samples showed a zincblende structure and the photoluminescence peak position depended on the surface to volume ratio of the films. There are also many research groups have reported TM-doped on wide band gap II-VI semiconductors [12-19] exhibiting room-temperature ferromagnetism. Saito *et al* [12] have reported room-temperature ferromagnetism and magneto-optical properties in a II-VI DMS of $Zn_{1-x}Cr_xTe$. Pan *et al* [13] report ferromagnetism in carbon-doped ZnO. Norberg *et al* [14,15] report the synthesis of colloidal Mn-doped ZnO quantum dots and the preparation of room-temperature ferromagnetic nanocrystalline thin films. Feng *et al* [16] have observed room-temperature ferromagnetism in $ZnFeO$ thin film. Twardowski *et al* [19] have reported the specific heat and low field susceptibility of $Zn_xFe_{1-x}S$ ($x<0.26$). But the Curie temperature T_c is very low (below 20K). However, up to date, there are few reports for high temperature ferromagnetism in Fe-doped cubic ZnS thin films.

On the other hand, the origin of ferromagnetism in DMS is still under debate. It is not clear if the TM-doped semiconductors will form TM clusters or secondary phases

[12-19]. In Ueda’s view [20] the low T_c of DMS results from either the low solubility of magnetic elements in the semiconductors or poor quality of DMS. A band structure model, based on the p - d and d - d level repulsions between the TM ions and host elements, has been successfully used to explain the magnetic ordering observed in all Mn-doped III-V and II-VI semiconductors [21]. In this model, the carriers (electrons or holes) play an important role in stabilizing the ferromagnetism of DMS. In order to confirm above model, we also perform first-principles calculations based on the local spin density approximations to study the magnetic properties of ZnS:Fe system. In this work, the $Zn_xFe_{1-x}S$ thin films are prepared by low-pressure metal-organic chemical vapor deposition (MOCVD) equipment on GaAs substrates. Structural and morphological studies are done by means of X-ray diffraction (XRD) technique using Cu K α irradiation on an 800 W Philips 1830 powder diffractometer. X-ray photoelectron spectroscopy (XPS) measurement is carried out on VG ESCALAB MK II instrument where Mg K α X-ray ($h\nu=1253.6$ eV) is used as the emission source. The magnetization measurements are performed by a Quantum Design superconducting quantum interference device (SQUID) system.

2. Experiments and theory

ZnS:Fe single-crystal thin films are grown on GaAs substrates by low-pressure MOCVD at substrate temperature of 350°C. The substrates are cleaned by ultrasonic with a sequence of trichloroethylene, acetone, ethanol and deionized (DI) water, and etched in the mixture solution of a $H_2SO_4:H_2O_2:H_2O=3:1:1$ at room temperature for 10min. Before put into the growth chamber, the chemical etched substrates are rinsed in DI water again and finally dried by nitrogen blowing. Precursors consist of ironpentacarbonyl

($\text{Fe}(\text{CO})_5$), dimethylzinc (DMZn) and H_2S . In our experiment, the growth pressure fixed is 76 Torr using a home-made horizontal reactor, and high purity hydrogen is used to carry the organometallics into the reaction chamber with the total gas flow rate of 21 min^{-1} . The GaAs substrate is cleaned in hydrogen ambient at 600°C 10min, which is demonstrated to be an effective method to remove the oxide layer and residual surface contaminants. Films are grown for 30min and the film thicknesses are about 200nm.

The Fe content in the reactor is controlled by varying the H_2 flow rate. The resulting Fe concentration in the sample is determined using XPS. The structure of the ZnS:Fe thin films is characterized by X-ray diffractometers. Surface morphology of the films is investigated by AFM operated in tapping mode. The high-temperature (100K) magnetic properties have been assessed using a SQUID magnetometer.

The calculations are performed using VASP code, based on the spin density functional theory. For the exchange and correlation potential, the generalized gradient approximation (GGA) is used. All plane waves with a cut-off energy of 300 eV are used in the basis function. For all the Fe-doped systems, a 64 atoms supercell is used for the defect calculations. The lattice constants of the supercells are kept fixed to that of pure ZnS. All the ion positions are allowed to relax until the forces on each of them become less than $0.02\text{eV}/\text{\AA}$. For ion relaxation, a $2\times 2\times 2$ Monkhost-Pack k -point sampling is used.

3. Results and discussion

The structure of ZnS:Fe thin film is examined by θ -2 θ X-ray diffraction system using $\text{CuK}\alpha$ radiation in the range 20° - 80° , which is shown in Fig.1. Firstly, strong $\text{Zn}_x\text{Fe}_{1-x}\text{S}$ (200) and (400) alloy peaks are observed at $2\theta=33.01^\circ$ and $2\theta=69.30^\circ$. GaAs substrates (200) and (400) peak are apparent near $2\theta=31.61^\circ$ and $2\theta=66.04^\circ$, respectively. No other peaks above the noise of the background are detected. From the Fig.1 rocking curve of ZnS (200) diffraction peak, it is clearly that the diffraction peaks indicate that ZnS single crystal grown on GaAs (200) substrate with cubic structure. And the ZnS:Fe thin film is phase pure with a (200) curve FWHM of 0.34 degrees. It can be explained that Fe ions substitute partly Zn ions and lead to the lattice structure difference. Addition, the X-ray diffraction results are comparable with those of ZnS films grown on Al_2O_3 sapphire substrates under the same conditions.[11] It is obviously shown that ZnS single crystal grown on $\text{Al}_2\text{O}_3(006)$ substrate is hexagonal structure, but the sample grown on GaAs(200) is cubic structure. The ZnS structure relates to the substrate and the Fe content, and the lattice structure is gradually changes from hexagonal to cubic structure under different substrates.

The fraction of Fe incorporated into the ZnS single-phase film is determined using X-ray photoelectron spectroscopy (XPS). Data of the XPS indicate the relative concentration of Fe to Zn to be 11% for this sample.

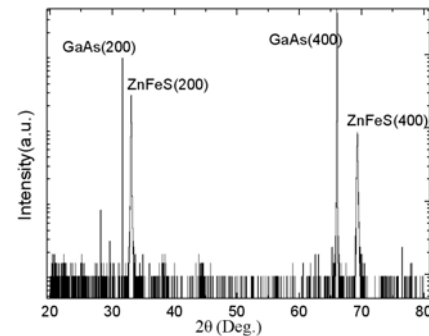


Fig. 1. XRD patterns for the Fe-doped ZnS thin film on the GaAs substrates.

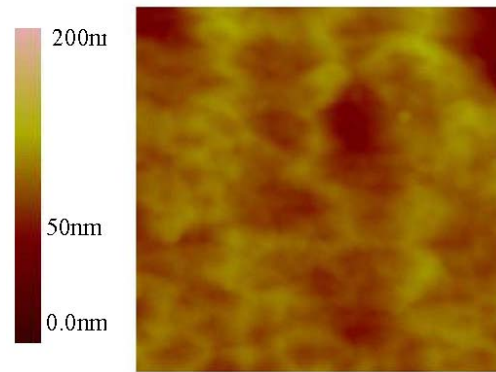


Fig. 2. (color online) AFM image of the Fe-doped ZnS film on GaAs.

AFM is used to investigate the effect of Fe doping on the ZnS single crystal thin film morphology. Single phase films are typically non-specular and exhibit large values for the root mean squared roughness, which shows in Fig.2. The morphology of the multi-phase films exhibits a much different morphology. A $2\text{nm} \times 2\text{nm}$ AFM micrograph for the Fe-doped ZnS thin films during the process of MOCVD is exhibited in Fig.2. The film thickness is 200nm and no precipitates like Fe cluster.

The temperature-dependent magnetization ($M-T$) curve for single-phase Fe-doped ZnS sample are measured using a SQUID magnetometer with a magnetic field of 1000Oe, applied perpendicular to the film plane. Measurements are taken at the relatively large applied magnetic field in order to increase the magnetic signal from thin film with respect to the large diamagnetic response of the GaAs substrate. Measurements have also been taken at 3000Oe and shown similar temperature dependence. The results of magnetization subtract of the diamagnetic contribution of the GaAs substrate. The *dc* zero-field-cooled (ZFC) and the field-cooled (FC) magnetization curves are shown in Fig.3. Measurements are performed from 5 to 300K. The FC is obtained by measuring the magnetic moment of the sample in a magnetic field of 1000 Oe during cooling. The ZFC measurement is obtained by first

cooling the sample to 5 K in zero fields and then warming it in the same field as that of the FC measurement. The ZFC magnetization shows stronger temperature dependence than the FC one below 30 K. ZFC and the FC magnetization curves are measured overlap after high temperature about 180K with a paramagnetic behavior. This temperature below which the ZFC-FC curves separate, the ferromagnetic ordering sets are shown clearly in Fig.3 [22, 23, 24]. Fig.3 displays a ferromagnetic behavior persisting up to 270K. Therefore, it obtains the Curie temperature T_c of 270K in this system. As seen in Fig.3 the sample displays ferromagnetic ordering and a decrease with increasing of temperature. Moreover, ferromagnetic transition temperatures of previous report are focus in other material. For example, A transition temperature more than room temperature is obtained in Fe-doped in ZnO:Cu reported by S.-J [25]. In the Co-doped ZnS samples, room-temperature magnetic hysteresis is observed [22]. But up to date, there is no work reporting Fe-doped ZnS thin film with high T_c of 270K grown by MOCVD.

Fig.4 displays the results of magnetization as a function of applied magnetic field measured for $Zn_xFe_{1-x}S$ film at 100K. The total magnetization could be described as an algebraic sum of various contributions. The substrate diamagnetic contribution is subtracted from the total magnetization signal. The remaining data consist of the paramagnetic and ferromagnetic contributions from the $Zn_xFe_{1-x}S$ thin film. The well-defined hysteresis loops show that the $Zn_xFe_{1-x}S$ film are clearly ferromagnetic at 100 K. At 100 K, the saturation magnetization (M_s) is 1.82×10^{-5} emu with a remanence magnetization (M_r) of 0.31×10^{-5} emu and a coercive field (H_c) of 50 Oe. GaAs substrate and ZnS are diamagnetic, so the magnetization data indicate that the ferromagnetism in the present study is because Fe-doped in ZnS thin film and formed $Zn_xFe_{1-x}S$ DMS.

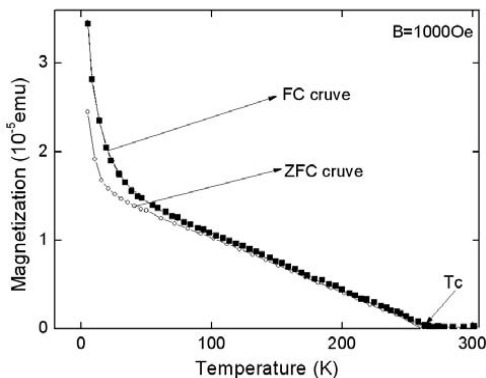


Fig. 3. The FC-ZFC M-T curve of the Fe-doped ZnS shows temperature-dependent magnetization of both zero-field-cooled (down - curve) and field-cooled (up - curve) in the field of 1.0 KOe.

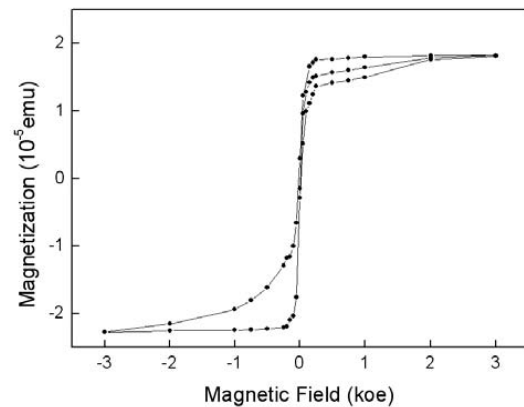


Fig. 4. M-H curve of the sample taken at 100 K after the necessary background diamagnetic subtraction, the magnetic field used is from 0 up to 0.3 T.

The origin of the ferromagnetism in DMS materials is still not clearly understood. To further demonstrate that the Fe-doped ZnS thin films are favorable for high temperature ferromagnetism , we model 64-atom cell to simulate the magnetic interactions of Fe atoms by performing first-principles spin-polarized density functional theory (DFT) calculations within generalized-gradient approximation (GGA). We can find that these magnetic interactions are mainly strong $p-d$ coupling between the Fe $3d$ states and S $2p$ states. The calculated total energy differences between ferromagnetic (FM) and anti-ferromagnetic (AFM) configuration ($\Delta E = E_{FM} - E_{AFM}$) are 46 meV, indicating that ferromagnetic ordering is favorable for ZnS:Fe system. Therefore, the observed ferromagnetism should be the intrinsic behavior of Fe-doped ZnS thin film.

4. Conclusions

In summary, we have reported the ferromagnetic properties of single-phase $Zn_xFe_{1-x}S$ thin films prepared on GaAs substrates by MOCVD as a new method. Field and temperature dependent magnetization curve indicated that a high curie temperature $T_c=270$ K. The XRD and AFM used for investigating the structural and surface characterization, the results indicated that no Fe clusters and other compounds are formed in the samples. The experimentally observed high T_c could be mainly ascribed to the p-d exchange coupling between Fe ions and host elements.

Acknowledgements

The authors would like to thank Professor Jingbo Li for enlightening discussions. This work is supported by the Postdoctoral Foundation under Contact No. O9T1050000.

References

- [1] H. Ohno, *Science* **281**, 951 (1998).
- [2] A. J. Mills, *Nature* **392**, 147 (1998).
- [3] J. M. D. Coey, M. Venkatesan, C. B. Fitzgerald, *Nature Mater.* **4**, 173 (2005).
- [4] A. Walsh, J. L. F. Da Silva, S.-H. Wei, *Phys. Rev. Lett.* **100**, 256401 (2008).
- [5] H. W. Peng, H. J. Xiang, S.-H. Wei, S. S. Li, J. B. Xia, J. B. Li, *Phys. Rev. Lett.* **102**, 017201 (2009).
- [6] H. X. Deng, J. B. Li, S. -S. Li, J. -B. Xia, A. Walsh, and S.-H. Wei, *Appl. Phys. Lett.* **96**, 162508 (2010).
- [7] T. Kryshchuk, V. S. Khomchenko, J. A. Andracca-Adame, V. E. Rodionov, V. B. Khachaturyan, Y. A. Tzyrkunov, *Superlattices and Microstructures* **40**, 651 (2006).
- [8] S. K. Mandal, S. Chaudhuri, A. K. Pal, *Thin Solid Films* **350**, 209 (1999).
- [9] Y. Q. Gai, J. B. Li, B. Yao, J. B. Xia, *J. Appl. Phys.* **105**, 113704 (2009).
- [10] J. Li, L. W. Wang, *Phys. Rev. B* **67**, 205319 (2003).
- [11] Q. J. Feng, D. Z. Shen, J. Y. Zhang, Y. M. Lu, Y. C. Liu, X. W. Fan, *Mater. Chem. Phys.* **96**, 158 (2006).
- [12] H. Saito, V. Zayets, S. Yamagata, K. Ando, *Phys. Rev. Lett.* **90**, 207202 (2003).
- [13] H. Pan, J. B. Yi, L. Shen, R. Q. Wu, J. H. Yang, J. Y. Lin, Y. P. Feng, J. Ding, L. H. Van, J. H. Yin, *Phys. Rev. Lett.* **99**, 127201 (2007).
- [14] N. S. Norberg, K. R. Kittilstved, J. E. Amonette, R. K. Kukkadapu, D. A. Schwartz, D. R. Gamelin, *J. Am. Chem. Soc.* **126**, 9387 (2004).
- [15] K. R. Kittilstved, D. R. Gamelin, *J. Am. Chem. Soc.* **127**, 5292 (2005).
- [16] Q. J. Feng, D. Z. Shen, J. Y. Zhang, B. H. Li, Z. Z. Zhang, Y. M. Lu, X. W. Fan, *Mater. Chem. Phys.* **112**, 1106 (2008).
- [17] X. Q. Meng, L. Tang, J. B. Li, *J. Phys. Chem. C*, (2010), in press.
- [18] L. Chen, S. Yan, P. F. Xu, J. Lu, W. Z. Wang, J. J. Deng, X. Qian, Y. Ji, J. H. Zhao, *Appl. Phys. Lett.* **95**, 182505 (2009).
- [19] A. Twardowski, H. J. M. Swagten, W. J. M. de Jonge, *Phys. Rev. B* **44**, 2220 (1991).
- [20] K. Ueda, H. Tabata, T. Kawai, *Appl. Phys. Lett.* **79**, 988 (2001).
- [21] G. M. Dalpian, S.-H. Wei, X. G. Gong, A. J. R. da Silva, A. Fazzio, *Solid State Commun.* **138**, 353 (2006).
- [22] S. Sambasivam, D. Paul Joseph, J.G.Lin, C.Venkateswaran, *Journal of Solid State Chemistry* **182**, 2589 (2009)
- [23] A. J. Blattner, B. W. Wessels, *Applied Surface Science* **221**, 155 (2004)
- [24] P. Poddar, Y. Sahoo, H. Srikanth, P. N. Prasad, *Appl. Phys. Lett.* **87**, 62506 (2005)
- [25] S.-J. Han, J. W. Song, C.-H. Yang, S. H. Park, J.-H. Park, Y. H. Jeong, K. W. Rhie, *Appl. Phys. Lett.* **81**, 4212 (2002)

^{*}Corresponding author: zhufeng@semi.ac.cn